Modeling Ionic Liquids Using a Systematic All-Atom Force Field

José N. Canongia Lopes*

Centro de Química Estrutural, Instituto Superior Técnico, Av. Rovisco Pais, 1049-001 Lisboa, Portugal

Johnny Deschamps and Agílio A. H. Pádua

Laboratoire de Thermodynamique. des Solutions et des Polymères, Université Blaise Pascal - 24 Av. des Landes, 63177 Aubière, France

Received: July 29, 2003; In Final Form: October 3, 2003

A new force field for the molecular modeling of ionic liquids of the dialkylimidazolium cation family was constructed. The model is based on the OPLS-AA/AMBER framework. Ab initio calculations were performed to obtain several terms in the force field not yet defined in the literature. These include torsion energy profiles and distributions of atomic charges that blend smoothly with the OPLS-AA specification for alkyl chains. Validation was carried out by comparing simulated and experimental data on fourteen different salts, comprising three types of anion and five lengths of alkyl chain, in both the crystalline and liquid phases. The present model can be regarded as a step toward a general force field for ionic liquids of the imidazolium cation family that was built in a systematic way, is easily integrated with OPLS-AA/AMBER, and is transferable between different combinations of cation−anion.

1. Introduction

Ionic liquids (ILs) are a class of organic salts with unusually low melting temperatures that attracted much attention from the scientific community in recent years. Apart from being liquid around room temperature, ionic liquids exhibit a negligible vapor pressure and interesting solvation or coordination properties that depend on the characteristics of the cation and anion. Their status as "green" or "designer" solvents explains the large amount of studies concerning their possible industrial use as reaction or extraction media.[1] Unfortunately, their thermophysical characterization is by no means extensive. The amount and scope of molecular modeling studies are also limited.[2−7]

In this article we introduce a force field to address three main issues. (i) Internal consistency. Many of the existing IL models borrow parameters from different, and not always compatible, sources: it is common to see parametrizations of the cation and the anion using information from different force fields. In this work ab initio calculations are used extensively to provide essential data for the development of an internally consistent force field. This includes molecular geometry optimization and the description of electron density using extended basis sets, leading to the evaluation of force field parameters such as torsion energy profiles and point charges on the interaction centers. (ii) Transferability. The parametrization of IL models should not be too specific because one wants to deal with families of similar compounds, generally the cations, that can be combined with different counterions. The proposed IL force field will concentrate on the parametrization of parts of the molecules that are common to an entire family of cations and adopts a strategy to add specific substituents. (iii) Compatibility. The model will build on the OPLS-AA force field.[8] This means that any molecule or residue already defined in the OPLS-AA database can be combined with the proposed force field. The choice of the OPLS-AA force field as a framework also benefits from its articulation with structural parameters from the even larger AMBER force field.[9]

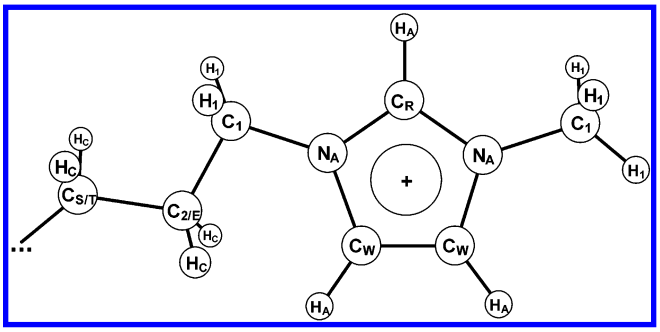

Figure 1. Nomenclature of the 1-alkyl-3-methylimidazolium cations. AMBER-like notation was used on the ring atoms.[9] C_1 refers to the first carbon atom in any side chain, C_E is the second carbon atom in the ethyl side chain of 1-ethyl-3-methylimidazolium, C_2 is the second atom in alkyl side chains with more than 2 carbon atoms, C_S refers to any secondary carbon of the alkyl side chain that is removed at least 2 bonds from the ring, and C_T is the terminal carbon atom of longer than ethyl side chains. H_A, H_1, and H_C refer to hydrogen atoms attached to the aromatic ring, to the first carbon atom on the side chains, and to carbon atoms on the side chain further removed from the ring, respectively. Abbreviations used for 1-alkyl-3-methylimidazolium cations are mim^+ = methylimidazolium, with prefixes a = alkyl, m = methyl, e = ethyl, b = butyl, h = hexyl, dd = dodecyl.

The most difficult point at this stage is the validation of any given IL model due to the scarce and sometimes inaccurate experimental data. Obviously, the present effort to achieve consistency does not necessarily guarantee accuracy. Despite the limited experimental data, the proposed force field will be tested against relevant experimental and simulation results from the literature.

The most extensively studied and modeled IL family has been that of the 1-alkyl-3-methylimidazolium cation (cf. Figure 1 for the atomic nomenclature adopted throughout this paper) with different counterions, PF_6^-, BF_4^-, Cl^-, etc. Because the

10.1021/jp0362133 CCC: $27.50
Published on Web 01/16/2004

TABLE 1: Available and Proposed Force-Field Models for Ionic Liquids

	model (authors)					
	HPLB [ref 2]	ABS [refs 3,5]	SBM [ref 4]	MM [ref 7]	MSB [ref 6]	CLDP [this work]
			Ions Modeled			
cations	$mmim^+$, $emim^+$	$emim^+$, $bmim^+$	$bmim^+$	$bmim^+$	$bmim^+$	$amim^+$, (C_1-C_{12})
anions	Cl^-, PF_6^-	$AlCl_4^-$, BF_4^-	PF_6^-	PF_6^-	PF_6^-	PF_6^-, Cl^-, NO_3^-
			Internal Geometry			
optimization						
level of theory	HF	UHF	RHF	B3LYP	HF	RHF
basis set	6-31G(d,p)	6-31G(d)	6-31G(d)	6-31G(d)	6-31G(d,p)	6-31G(d)
electron density						
level of theory	MP2	UHF	RHF	B3LYP	HF	MP2
basis set	6-31G(d,p)	6-31G(d)	6-31G(d)	6-311+G(d)	6-31G(d,p)	cc-pVTZ(-f)
partial charges	DMA	RESP	CHelpG	CHelpG	ESP	CHelpG
			Internal Force Field			
cation ring[a]	rigid	AMBER	rigid	CHARMM	OPLS-AA	OPLS-AA
cation alkyl chain	free dihedrals	AMBER	OPLS-UA, OPLS-AA dihedrals	CHARMM	OPLS-AA	OPLS-AA, estd by QM/MM
anion	rigid	estd by QM/MM	one center	estd by QM	rigid	rigid
			External Force Field			
parametrization	Exp6 + q	LJ + q	LJ + q	LJ + q	LJ + q	LJ + q
cations	Williams	AMBER	OPLS-UA	CHARMM	OPLS-AA	OPLS-AA
anions	Williams, MMFF94	AMBER, DREIDING	SF_6 data	CHARMM	OPLS-AA	OPLS-AA, AMBER
	MD method	MD method	MC method	MD method	MD method	MD method
initial cell geometry	CCDB, private comm. (crystal), random (fluid)	grid with randomly positioned ions (fluid)	random (fluid)	random (fluid)	expanded lattice, random (fluid)	CCDB (crystal), expanded lattice, random (fluid)
production length	5 × 100 ps	100 ps	2 × 5000 cycl	4 ns	20 × 50 ps	150−350 ps
			Validation			
internal analysis	RDF, energy	RDF, energy	RDF, energy	RDF, energy	RDF	energy
experimental data	crystal structures, density	neutron scattering, density, self-difusion	density, α_p, β_T	IR data, density, α_p, β_T, self-difusion	self-difusion	crystal structures, density

[a] The five atoms in the ring plus the five atoms directly attached to them.

validation of the molecular model is always a primary concern, the development of the present IL model will focus on the family of this particular cation and some of the most common anions.

2. Force Field Development

The parametrization of a force field and its validation using simulation techniques requires the knowledge of four sets of molecular data: (i) molecular geometry; (ii) intramolecular force field, applicable in the case of nonrigid molecules; (iii) crystalline geometry, applicable in the case of simulations of ordered phases; and (iv) intermolecular potential. The first two sets comprise internal molecular parameters that can be estimated from quantum mechanical calculations and/or gas-phase spectroscopic data whereas the last two sets include external or intermolecular parameters to be inferred from auxiliary diffraction and/or bulk thermodynamic data. Sets ii and iv contain the so-called force field parameters.

The currently available IL force field models used different approximations to build each set of parameters. The differences and similarities are summarized in Table 1 along with the model developed in this paper.

Molecular Geometry. The molecular geometry parameters are generally obtained from low-level ab initio calculations using a simple basis set describing a single molecule (cf. Results section below). All the models under discussion used a similar method to estimate the parameters describing the imidazolium ring (bond lengths, angles, and dihedrals) and the published results are comparable with experimental data obtained by diffraction studies, as shown in Table 2. Two conclusions can be drawn directly from the table: (i) the ring geometry is not strongly affected by the environment of the imidazolium molecule because the ring geometries in two completely different crystals, [emim][$VOCl_4$] and [ddmim][PF_6],[21,22] are comparable between them and similar to the ab initio values for the isolated imidazolium cation, and (ii) the distortion of the ring caused by different alkyl substituents is so small that the use of a symmetrical ring geometry as in a $mmim^+$ cation represents a good approximation.

In fact, the geometry of the imidazolium cation ring can be qualitatively rationalized if one compares it with the isoelectronic structures of the cylclopentadienyl anion, pyrrole, and imidazole, as shown in Figure 2. Whereas the cylclopentadienyl anion is a regular pentagon with average C−C distances around 139 pm,[10] the imidazolium ring is somewhat smaller and slightly deformed due to the shorter N−C bonds and to the presence of nonequivalent contributors to the resonance hybrid. In the imidazolium cation the N_A-C_W distances (around 138 pm) are comparable to the N−C distance in pyrrole (137.8 pm) and correspond to a single bond; the C_W-C_W distances (134.1 pm) are characteristic of C−C double bonds (134 pm); and the short N_A-C_R distances (131−132 pm) represent a "one-and-an-half" N−C bond.

The internal angles on the imidazolium ring do not deviate significantly from the regular pentagon angle of 108°: the C_R tip is somewhat less acute (109.8°), and the C_W tips compensate that distortion by being more acute (107.1°). The other small but noticeable distortion is on the angles to the atoms connected at N_A and C_W. For instance, the angle between the alkyl side chains and the C_R atom ($C-N_A-C_R$ angle) are always slightly larger than the angle to the C_W atom ($C-N_A-C_W$ angle).

All dihedrals on the imidazolium ring calculated from ab initio methods are approximately either 0° or 180° so the ring and the atoms directly connected to it are on the same plane. This is not always true in the case of experimental diffraction data

TABLE 2: Molecular Geometry of the 1-Alkyl-3-methyl-imidazolium Cation Family and the PF_6^- and NO_3^- Anions[a]

	$emim^+_{XR}$[b] [ref 21]	$ddmim^+_{XR}$[c] [ref 22]	$emim^+_{AI}$ [ref 3]	$emim^+_{AI}$[d] [ref 4]	$amim^+_{AI}$[e] [this work]
			Bonds (Å)[f]		
N_A-C_R	1.311(4)	1.322(3)	1.326(3)	1.314	**1.315**
	1.311(4)			1.315	
N_A-C_W	1.357(5)	1.373(3)		1.378	**1.378**
	1.360(6)	1.374(3)		1.378	
C_W-C_W	1.334(8)	1.334(8)		1.342	**1.341**
N_A-C_1	1.452(4)	1.468(3)		1.466	**1.466**
	1.468(4)	1.477(3)		1.478	
C_1-C_E	1.500(9)			1.520	
			Angles (deg)[f]		
$N_A-C_R-N_A$	109.6(3)		109.8	109.9	**109.8**
$N_A-C_W-C_W$	107.1(3)		108.1	107.0	**107.1**
	107.6(4)		108.0	107.2	
$C_W-N_A-C_R$	108.0(3)		106.9	107.9	**108.0**
	107.6(2)		106.8	108.0	
$C_W-N_A-C_1$	125.9(3)			125.6	**125.6**
	125.2(3)			125.9	
$C_R-N_A-C_1$	126.5(3)			126.4	**126.3**
	125.4(3)			126.1	

	$PF_6^-{}_{XR}$[g] [ref 23]	$PF_6^-{}_{XR}$[b] [ref 22]	$PF_6^-{}_{AI}$ [ref 24]	$NO_3^-{}_{XR}$[h] [ref 25]	$NO_3^-{}_{AI}$ [ref 26]
			Bonds (Å)		
P−F	1.566	1.596	**1.560**		
N−O				1.220	**1.250**

[a] Comparison between experimental crystal X-ray (XR) geometries and single-molecule ab initio (AI) calculations. The results in bold are those used in the parametrization of the present force field [b] [emim][$VOCL_4$] crystal. [c] [ddmim][PF_6] crystal. [d] Calculated from molecular coordinates given in the reference. [e] Average values, valid for an imidazolium ring with any alkyl susbstituent. [f] Double entries refer to bond lengths and angles on the alkyl and methyl side of the imidazoilum ring, respectively. [g] [emim][PF_6] crystal. [h] [emim][NO_3] crystal.

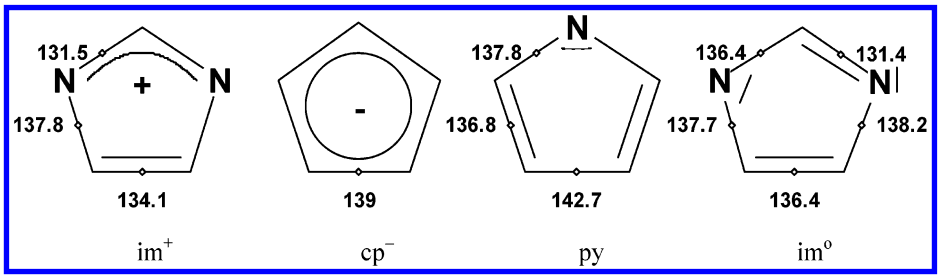

Figure 2. Geometry of the imidazolium cation (im^+), cyclopentadienyl anion (cp^-), pyrrole (py), and imidazole (im°) rings. All bond distances are in picometers. The lines inside each ring represent the delocalized π-electrons in the corresponding aromatic systems. The four π-electrons predominantly shared between three atoms in im^+ and the six π-electrons shared between five atoms in cp^- are shown as curved lines. The lone pair of electrons in one of the nitrogen atoms in im° is also shown.

where the crystal geometry can impose slight out-of-the-plane distortions on the atoms connected to the ring.[22]

The geometry of the alkyl side chains (C−C and C−H bond lengths, H−C−H, C−C−C, and C−C−H angles) are similar to those found in normal aliphatic chains. The carbon in the side chain connected to the N_A atom is counted as part of the ring and not as a proper member of the side chain.

To establish the molecular geometry of the PF_6^- and NO_3^- anions (taken as octahedral and planar triangular structures, respectively), it is sufficient to know the P−F and N−O interatomic distances. These were taken from ab initio data[24,26] and are also presented in Table 2. The corresponding distances obtained from X-ray diffraction studies in selected IL crystals compare favorably with the ab initio results.

Intramolecular Force Field. Many bond, angle, and dihedral parameters used in this work were taken from or based on the OPLS-AA and AMBER force fields, which are largely compatible with respect to the intramolecular terms. Whenever we found significant differences between our ab initio geometries and OPLS-AA or AMBER parameters, notably in equilibrium distances and angles, we proposed new values, reported in Table 3. We did not modify force constants from what is specified in AMBER and OPLS-AA, because these features have a relatively small effect on thermodynamic properties.

The force field parameters were developed using a procedure similar to previous studies concerning heterocyclic five-membered rings.[28] Because the OPLS-AA/AMBER database does not contain information about the imidazolium cation itself, the bond lengths of the ring were chosen to reproduce the ab initio geometry of the isolated cations (see previous section) whereas the relevant stretching and bending force constants of the ring were inferred from the values published for similar heterocyclic compounds such as imidazole, pyrrole, and purines.[9,28,29] The main departure from the OPLS-AA force field at this point regards our use of constrained bond lengths for all C−H stretching modes present in the cations (cf. Results section below).

Margulis et al.[6] also used OPLS-AA/AMBER parameters to define the internal force field of the 1-butyl-3-methylimidazolium cation but chose to model the ring directly with imidazole parameters (neutral and asymmetric ring). The same applies to the work of de Andrade et al.:[5] although the CHARMM force field contains parametric data concerning the protonated histidine ring, the authors chose parameters that can be understood

TABLE 3: 1-Alkyl-3-methylimidazolum Force-Field Parameters[a]

atoms	q (e)	σ (Å)	ϵ (kJ mol^{-1})	C1	C2	C4	C6	C12	C18	source
C_1	−0.17	3.50	0.27614	2	2	2	2	2	2	this work (q), OPLS (butane)[8]
C_2	0.01	3.50	0.27614			1	1	1	1	this work (q), OPLS (butane)[8]
C_E	−0.05	3.50	0.27614		1					this work (q), OPLS (butane)[8]
C_R	−0.11	3.55	0.29288	1	1	1	1	1	1	this work (q), OPLS (HIP[d])[27]
C_S	−0.12	3.50	0.27614			1	3	9	15	OPLS (butane)[8]
C_T	−0.18	3.50	0.27614			1	1	1	1	OPLS (butane)[8]
C_W	−0.13	3.55	0.29288	2	2	2	2	2	2	this work (q), OPLS (HIP[d])[27]
H_A	0.21	2.42	0.12552	3	3	3	3	3	3	this work (q), OPLS (HIP[d])[27]
H_C	0.06	2.50	0.12552		3	7	11	23	35	OPLS (butane)[8]
H_1	0.13	2.50	0.12552	6	5	5	5	5	5	this work (q), OPLS (butane)[8]
N_A	0.15	3.25	0.71128	2	2	2	2	2	2	this work (q), OPLS (HIP[c])[27]

bonds	r_{eq} (Å)	K_r (kJ mol^{-1} Å^{-2})	C1	C2	C4	C6	C12	C18	source
$C_{R/W}-H_A$	1.08	(constrained)	3	3	3	3	3	3	OPLS (imidazole)[28]
C*−H* [b]	1.09	(constrained)	6	8	12	16	28	40	OPLS (butane)[8]
C_R-N_A	1.315	1996	2	2	2	2	2	2	this work (r), OPLS (imidazole)[28]
C_W-N_A	1.378	1787	2	2	2	2	2	2	this work (r), OPLS (imidazole)[28]
C_W-C_W	1.341	2176	1	1	1	1	1	1	this work (r), OPLS (imidazole)[28]
N_A-C_1	1.466	1410	2	2	2	2	2	2	this work (r), AMBER(N*-CT)[9,29]
C*−C* [b]	1.529	1121		1	3	5	11	17	OPLS (butane)[8]

angles	θ_{eq} (deg)	K_θ (kJ mol^{-1} rad^{-2})	C1	C2	C4	C6	C12	C18	source
$C_W-N_A-C_R$	108.0	292.6	2	2	2	2	2	2	this work (θ), OPLS (imidazole)[28]
$C_W-N_A-C_1$	125.6	292.6	2	2	2	2	2	2	this work (θ), OPLS (imidazole)[28]
$C_R-N_A-C_1$	126.4	292.6	2	2	2	2	2	2	this work (θ), OPLS (imidazole)[28]
$N_A-C_R-H_A$	125.1	146.3	2	2	2	2	2	2	this work (θ), OPLS (imidazole)[28]
$N_A-C_R-N_A$	109.8	292.6	1	1	1	1	1	1	this work (θ), OPLS (imidazole)[28]
$N_A-C_W-C_W$	107.1	292.6	2	2	2	2	2	2	this work (θ), OPLS (imidazole)[28]
$N_A-C_W-H_A$	122.0	146.3	2	2	2	2	2	2	this work (θ), OPLS (imidazole)[28]
$C_W-C_W-H_A$	130.9	146.3	2	2	2	2	2	2	this work (θ), OPLS (imidazole)[28]
N_A/C*−C*−H* [b]	110.7	313.2	6	10	18	26	50	74	OPLS (butane)[8]
N_A/C*−C*−C* [b]	112.7	418.4		4	3	5	11	17	OPLS (butane)[8]
H*−C*−H*	107.8	276.1	6	4	9	11	17	23	OPLS (butane)[8]

dihedrals	V_1 (kJ mol^{-1})	V_2 (kJ mol^{-1})	V_3 (kJ mol^{-1})	C1	C2	C4	C6	C12	C18	source
$X-N_A-C_R-X$	0	19.46	0	8	8	8	8	8	8	AMBER[9]
$X-C_W-C_W-X$	0	44.98	0	4	4	4	4	4	4	AMBER (X−CC−CW−X)[9]
$X-N_A-C_W-X$	0	12.55	0	8	8	8	8	8	8	AMBER[9]
$C_W-N_A-C_1-H_1$	0	0	0.55	6	5	5	5	5	5	this work
$C_R-N_A-C_1-H_1$	0	0	0	6	5	5	5	5	5	this work
$C_W-N_A-C_1-C_{2/E}$	−5.76	4.43	0.877		1	1	1	1	1	this work
$C_R-N_A-C_1-C_{2/E}$	−3.23	0	0		1	1	1	1	1	this work
$N_A-C_1-C_2-C_{S/T}$	0.738	−0.681	1.02			1	1	1	1	this work
$N_A-C_1-C_{2/E}-H_C$	0	0	0		3	2	2	2	2	this work
C*−C*−C*−H*	0	0	1.531			9	17	39	63	OPLS (butane)[8]
H*−C*−C*−H*	0	0	1.331		6	14	22	48	72	OPLS (butane)[8]
C*−C*−C*−C*	0.728	−0.657	1.167			1	3	9	15	OPLS (butane)[8]
$X-N_A-X-X$ [c]	0	8.37	0	4	4	4	4	4	4	AMBER (X−N*−X−X)[9]
$X-C_{W/R}-X-X$ [c]	0	9.2	0	6	6	6	6	6	6	AMBER[9,29]

[a] C1 to C18 represent the number of occurrences of each term in a given amim cation designated by the number of carbons in the longer side chain. [b] No difference found in the equilibrium angles and force constants of aliphatic carbons connected either to carbon or nitrogen. C* represents a generic aliphatic carbon, C_1, C_2, C_E, C_S, or C_T. H* represents either H_1 or H_C. [c] Improper dihedral. [d] HIP is the protonated histidine cation.

as averages of the two (asymmetrical) halves of the neutral histidine ring. Unlike the imidazolium ring, the imidazole ring residue is not symmetrical and the distortions of the structure around the carbon connected to the two (nonequivalent) nitrogen atoms are noticeable (cf. distances around C_R in imidazole in Figure 2). The use of imidazole bond distances and angles to define an imidazolium cation can lead to an inaccurate parametrization.

In the present work, the stretching and bending force constants related to the bonds between the ring and the alkyl side chains were taken from AMBER parameters used to model similar bonds in purines (adenine and guanine included in nucleic acids).[9] It should be noted that the OPLS-AA force field adopts the same force constants when modeling the bonds and angles involving the N−C pair in amines and amides.[27] The corresponding values, both force constants and distances, for the alkyl side chains were taken from the OPLS-AA publication covering aliphatic chains.[8] The parameters defining the torsion energy profiles in the imidazolium ring were taken from the AMBER force field concerning heterocyclic aromatic molecules. These include the improper dihedrals needed to maintain the ring and the atoms directly attached to it in a planar geometry. The OPLS-AA specification of five-membered heterocyclic aromatic rings[28] constrained the ring and the atoms directly connected to it to be planar, which means that no dihedrals involving those atoms needed to be defined. Nevertheless, the authors of OPLS-AA recommend the use of AMBER parameters for cases where there are no ad-hoc constraints. The torsion profiles along the aliphatic side chain were obtained from the published OPLS-AA results.[8] The missing parameters corresponding to the dihedrals between atoms belonging to the imidazolium ring and those in the alkyl side chain were defined in this work with the aid of ab initio calculation (cf. Results).

As regards the anions simulated in this work, they were modeled as rigid molecules. No intramolecular force field parametrization is therefore needed, apart from the interatomic distances given in the previous section. Of course one might object that, because the cations were modeled as flexible molecules, we should have used a similar approach when dealing with the anions. Two facts justify our present choice: (i) The anions under discussion are not articulated molecules (there are no proper dihedral angles involved). This means that using fixed bond lengths and angles will not hinder any internal movement of the molecule. And (ii) there is a large uncertainty associated with the parametrization of the external force field of these ions; cf. Intermolecular Potential section below. In our opinion the use of a more complete internal force field is not relevant at this stage, before these (and other) anions have a better defined set of external parameters.

Crystal Geometry. The ionic liquids based on the 1-alkyl-3-methylimidazolium cation family exhibit higher melting-point temperatures for cations with either very short or long alkyl side chain lengths: $mmim^+$ and $emim^+$ with Cl^-, PF_6^-, or NO_3^- and also [ddmim][PF_6] have melting points above 273 K. The crystalline structures of these salts are documented at the Cambridge Crystallographic Database and can be used to validate the force field parametrization. Such a procedure was used by Hanke et al.[2] to test their model describing the above-mentioned $mmim^+$ and $emim^+$ salts. In the present work the prediction of the crystalline structure using the proposed force field is extended to salts containing the $ddmim^+$ cation and the nitrate anion. The crystallographic data needed to establish the structure of each salt will be given along with the simulation results (cf. Results).

TABLE 4: Lennard-Jones Parameters and Atomic Charges for Selected IL Anions

atoms	q (e)	σ (Å)	ϵ (kJ mol^{-1})	source
P, PF_6^-	1.34	3.7400	0.8368	OPLS[24]
F, PF_6^-	−0.39	3.1181	0.2552	OPLS[24]
N, NO_3^-	0.95	3.0600	0.3380	fit to Born−Mayer[11] + q_{AI}[11]
O, NO_3^-	−0.65	2.7700	0.6100	fit to Born−Mayer[11] + q_{AI}[11]
Cl, Cl^-	−1.00	3.7700	0.6200	fit to Born−Mayer[12]

Intermolecular Potential. The OPLS-AA/AMBER external force fields both comprise repulsion−dispersion terms parametrized by a 12−6 Lennard Jones potential function and an electrostatic term represented by partial charges located at each interaction site of the molecule.

In the case of the imidazolium cations, the Lennard-Jones parameters for each type of atom were taken from the OPLS-AA parametrization of heterocyclic aromatic rings[28] or aliphatic compounds[8] (Table 3). The interactions between atoms of different type were parametrized using the Lorentz−Berthelot mixing rules (arithmetic and geometric mean rules for σ and ϵ, respectively). The partial charges on each atom were calculated from the electron density obtained by ab initio calculation, using an electrostatic surface potential methodology (cf. Results).

The partial charges and Lennard-Jones parameters in the PF_6^- anion were taken directly from the OPLS-AA force field.[24] The NO_3^- ion was modeled by four Lennard-Jones centers whose parameters were determined by fitting to the Born−Mayer potential used to describe dispersive interactions in molten salts.[11] The partial charges had been calculated ab initio. The parameters for Cl^- were obtained in a similar way, fitting to the Born−Mayer potentials developed for crystalline and molten salts.[12] At this point it is important to stress that the resulting Lennard-Jones parameters for Cl^- are quite different from those usually employed for chlorine atoms bonded to organic molecules or aqueous Cl^-. The differences are apparent if we compare the interaction diameter, σ, in the three situations: 3.77 Å in molten salts/ionic crystals,[12] around 3.5 Å in organic chlorine atoms,[2,8,9] and around 4.4 Å in aqueous solution.[9] All intermolecular parameters concerning the anions presented in this work are compiled in Table 4.

3. Results

Ab Initio Calculations of Torsion Energy Profiles. New torsion potentials corresponding to dihedral angles between the imidazolium ring and the alkyl side chains were developed following a procedure similar to the one adopted for the OPLS-AA force field.[8,13] They were obtained from relaxed potential energy scans at a series of values for the dihedral angles of interest, which were held fixed while the remaining internal coordinates of the molecule were allowed to relax to energy minima.

Quantum chemical calculations were performed using Gaussian 98[14] at the MP2/cc-pVTZ(-f)//HF/6-31G(d) level of theory, thus using the same basis set as in the recent OPLS-AA model for perfluoroalkanes.[13] The cc-pVTZ(-f) basis set[15] was used for single-point energy calculations in geometries optimized at the HF/6-31G(d) level, as is current practice in the development of force field parameters for molecular simulation.[9,16] We used frozen-core MP2 calculations instead of the local MP2 method used by Watkins and Jorgensen.[13] The differences between the two methods are small.[17] For the C and N atoms the cc-pVTZ(-f) basis set is created by removing the *f* functions from the definition of the triple-ζ cc-pVTZ basis set of Dunning.[15] The combination of the levels of theory and basis sets used here

has been tested on a large collection of molecules (Halgren test) and was demonstrated to yield accurate conformational energetics.[18]

The torsion potential energy profiles depending on dihedral angles associated with each chemical bond of interest were described, for the purpose of molecular simulation, by cosine series of the form adopted in OPLS-AA.[8] The parameters developed in this work correspond to the dihedral angles $C_R-N_A-C_1-H_1$ and $C_W-N_A-C_1-H_1$ (fitted to torsion energy profiles for $mmim^+$), $C_R-N_A-C_1-C_{2/E}$, $C_W-N_A-C_1-C_{2/E}$, and $N_A-C_1-C_{2/E}-H_C$ (fitted to torsion energy profiles for $emim^+$), and $N_A-C_1-C_2-C_3$ (fitted to torsion energy profiles for $bmim^+$). This building up method ensures compatibility of the different dihedral functions and allows the description of a homologous series of molecules.

The calculation of the coefficients of the cosine series is not possible by direct adjustment to the ab initio energy profiles. This complication is due to the presence of nonbonded interactions in the force field that must be accounted for. In fact, in the specification of the OPLS-AA force field, sites within the same molecule separated by more than three bonds interact by Lennard-Jones and electrostatic potentials scaled by a factor of 0.5.[8] Sometimes these nonbonded interactions contribute with a large part of the torsion energy. This means that in the force field, the dihedral functions need not account for the whole torsion energy profiles, because there are contributions from "steric" effects due to the nonbonded interactions.

The values of the coefficients in the cosine series were found by a fitting procedure requiring structure optimizations with the force field models, performed by molecular simulation of isolated molecules. These MD calculations are done in two steps.[17] First, the geometry of each conformer, for a given constrained value of the dihedral angle, was optimized using molecular simulation with the coefficients of the dihedral function being adjusted set to zero; i.e., the contribution to the torsion energy from that particular dihedral angle came only from nonbonded interactions. After a full scan of the dihedral angle under study is performed, the role of the cosine series will be to correct the torsion profile thus obtained to match the one that resulted from the ab initio calculations described above. Therefore, the dihedral coefficients were adjusted, by least squares minimization, to the differences between the ab initio energy profiles and those calculated using this incomplete force field.

The simulation procedure employed to optimize the geometries consisted of a series of molecular dynamics quench runs on an isolated molecule, during which 10 000 time steps of 0.5 fs were simulated at each of the following temperatures: 10, 1, 0.1, and 0 K. The dihedrals being scanned were constrained at the desired angles by the addition of very steep harmonic terms where necessary.[17] In all cases the range of interest for a given dihedral angle was scanned at 10° intervals, to mimic the set of ab initio calculations. Computer simulations were carried out using the DL_POLY package.[19] The energy of the isolated molecule in its optimized configuration, in which all other torsions, as well as all bonds and all valence angles, where allowed to relax toward a conformational energy minimum, corresponds to one point in the torsion energy profile, for the constrained value of the dihedral being scanned. This procedure is not identical, in terms of the techniques or software tools used, to those employed in the development of OPLS-AA but was validated in a previous work.[17]

Once in possession of the adjusted coefficients of the cosine series, the procedure above is repeated, but now with the full dihedral functions, enabling us to verify that the complete force field actually yields the same torsion energy profile as the ab initio calculations, as seen in Figure 3. We prefer to employ this procedure of relaxed scans using the force field rather than imposing the equilibrium conformations obtained in the ab initio geometry optimizations. Our choice avoids straining the intramolecular terms such as bond lengths, valence angles, and remaining dihedrals, which might not be all perfect matches between the force field and the quantum results. The torsion energy profiles that we develop arise from structure optimizations within the force field itself, using molecular simulation, and this situation corresponds closely to the final use intended for the model, which is the simulation of fluid phases.

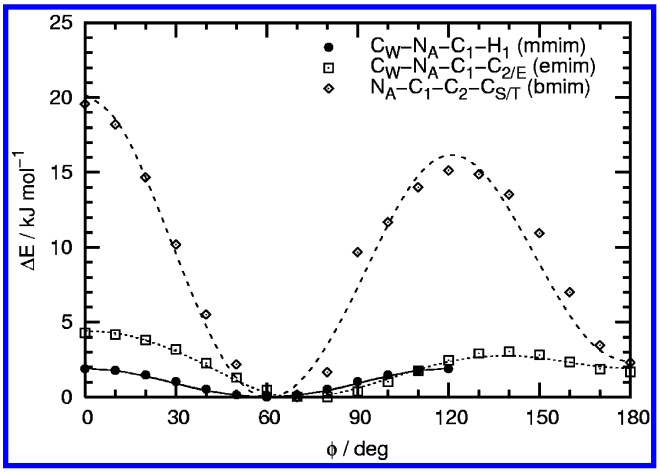

Figure 3. Torsion profile of the dihedrals involving imidazolium ring to aliphatic side chain bonds in 1-alkyl-3-methylimidazolium cations.

The parameters obtained in the present study are collected in Table 3, and a plot of some of the torsion energy profiles and of the representation of the ab initio energies by the force field, is given in Figure 3. The present numerical coefficients were calculated specifically for the imidazolium cation family, using the building up procedure explained above, whenever parameters were not available in OPLS-AA or AMBER. A comparison between the values we obtained here and those of other force fields for imidazolium cations follows. For the dihedral $C_W-N_A-C_1-H_1$, Morrow and Maginn[7] (MM) and de Andrade, Böes, and Stassen[3,5] (ABS) set all coefficients to zero, whereas Margulis, Stern, and Berne[6] (MSB) give a value of $V_3 = 2.34$ kJ mol^{-1}, which is much larger than ours (for nitrogen atoms, instead of type NA, these authors seem to employ parameters for nitrogen atoms of the type NB, which in AMBER notation are nitrogens in five-membered rings with a lone pair). For the dihedral $C_W-N_A-C_1-H_1$, MM use a nonzero V_2 coefficient, ABS set all to zero, and MSB give a value for V_3 larger than ours. The rotational barrier associated with the methyl groups in $mmim^+$, obtained both by ab initio means and with our parameters, is shown in Figure 3.

For the dihedral $C_W-N_A-C_1-C_2$, MM give a positive V_1 coefficient, ABS set this term to zero (according to the AMBER values for generic X−N*−CT−X), and MSB have negative V_1 and V_2 coefficients. For the closely related $C_R-N_A-C_1-C_2$ dihedral, MM give a small, negative V_1 coefficient, ABS set this to zero (AMBER values for generic X−N*−CT−X), and MSB keep the same negative V_1 and V_2 coefficients as for $C_W-N_A-C_1-C_2$. These two functions make up a very important contribution to the torsion energy of the cation. They are correlated by an angle of 180° because of the ring geometry, because C_R and C_W are both connected to the nitrogen atom. So these two functions were fitted simultaneously by us, and

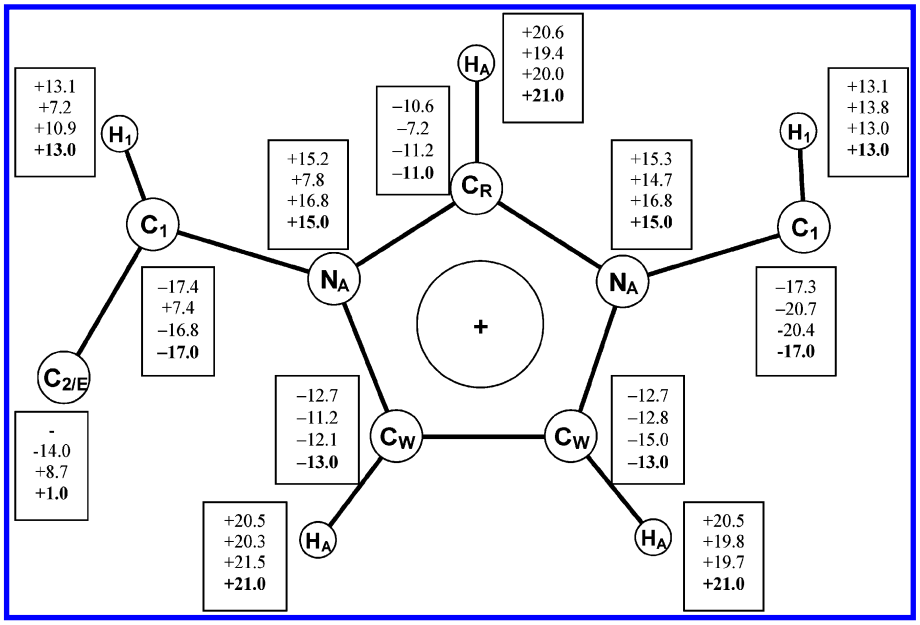

Figure 4. Atomic partial charges of the imidazolium ring and adjacent atoms. All numbers are percentage values of the charge of one proton. The other carbon and hydrogen atoms in the alkyl side chain (not shown) were given OPLS-AA charges. The list at each atom corresponds to the charge values obtained from ab initio calculations for $mmim^+$, $emim^+$, and $bmim^+$ and (in bold) the value adopted in the present force field, respectively.

the values found for the parameters of both dihedral functions are mutually different, as can be seen in Table 3.

Finally, for dihedral $N_A-C_1-C_2-C_T$, MM set it to zero, ABS use AMBER values for generic X−CT−CT−X, and MSB adopt coefficients much larger than ours, taken from OPLS-AA for aliphatic amines. In the case of $N_A-C_1-C_2-H_C$ we obtained negligible coefficients, MM also set this term to zero, and ABS use AMBER values for generic X−CT−CT−X, whereas MSB adopt again large coefficients, taken from OPLS-AA for aliphatic amines.

In conclusion to this section, we justify the effort undertaken here, for the first time to our knowledge, to calculate in a rigorous manner the dihedral terms affecting the junction between the aromatic ring and the alkyl side chain for the family of imidazolium cations. The force fields proposed in the literature so far contain some crude approximations and guesswork in this particular aspect, which certainly affect the conformational details of the ionic liquids.

Ab Initio Calculation of Partial Charges. Atomic charges on the imidazolium ring and its adjacent atoms were also obtained in the present study. They were calculated for $mmim^+$, $emim^+$, and $bmim^+$ by electrostatic surface potential fits, using the CHelpG procedure,[20] to electron densities obtained at the MP2/cc-pVTZ(-f) level. For $emim^+$ and $bmim^+$ the charges correspond to the average of two different geometries at conformational energy minima. The results are shown in Figure 4. To ensure the transferability of the model along the entire dialkylimidazolium cation family: (i) The charges on the atoms of the ring, those directly attached to it and the H_1 hydrogen atoms, were given symmetrical values along the C_{2v} axis of the ring and have values close to those found for $mmim^+$. For $bmim^+$ and $emim^+$ the differences, including departures from symmetry, are small; cf. Figure 4. (ii) The charges on all atoms in the alkyl side chain removed from the ring more than 3 bonds (C_S or C_T and H_C) were given the corresponding OPLS-AA values for alkanes;[8] (iii) The charge in the remaining atom that establishes the connection between the ring and the side chain, C_E in $emim^+$ and C_2 in longer side chains, was found empirically to respect the total charge of the cation. The values of the adopted charges are listed in Table 3 and compared with results from other force fields in Table 5.

Although we performed calculations on a larger basis set and employed a method including electron correlation (MP2), the charges obtained in this work show an overall agreement with those proposed by several other authors that used electrostatic surface potential fits to the ab initio electron densities. An exception is the relative charge distribution between the nitrogen atoms and carbon atom between them: our N_A atoms are somewhat more positive and this is compensated by a less positive C_R atom. The distributed multipole analysis method employed by Hanke et al.[2] yielded a significantly different set of atomic charges, in both sign and magnitude, when compared with all other authors.

MD Simulations. The validation of the proposed force field was based on simulation results obtained using the molecular dynamics technique, implemented with the DL_POLY software.[19] The strategy was simple: because the most accurate and common experimental data concerning ILs are densities, we decided to test the performance of the proposed force field in the estimation of molar densities along the family of the imidazolium cation, with different counterions, in both the crystalline and liquid phases.

Crystalline Phase. Five crystalline structures containing the imidazolium cation were selected from the Cambridge Crystallographic Database (CCDB). These were the sole $mmim^+$-based structure found in the database ([mmim][Cl]), three of the more than thirty $emim^+$-based structures ([emim][Cl], [emim][NO_3], and [emim][PF_6]), and a $ddmim^+$ structure ([ddmim][PF_6]). For 1-alkyl-3-methylimidazolium cations with alkyl side chains ranging from three to eleven carbon atoms there are very few crystallographic structures recorded at the CCDB, all of them including large or heavy counterions. This fact reflects the low melting point temperatures of imidazolium ILs with intermediate side-chain length; see Discussion section.

The simulation boxes and initial configurations were set by taking into account the dimensions and occupancy of the unit cells of each crystalline structure. Because the dimensions of the unit cells of these crystals are too small to accommodate a

TABLE 5: Charge Distribution in 1,3-Alkylmethylimidazolium Cations According to Different Force Fields[a]

	model (authors)												
	HPLB [ref 2]		ABS [refs 3,5]			SBM [ref 4]		MM [ref 7]		MSB [ref 6]		CLDP this work	
Ions Modeled													
cations	$mmim^+$, $emim^+$		$emim^+$ $bmim^+$			$Bmim^+$		$bmim^+$		$bmim^+$		$amim^+$ (C_1-C_{12})	
Method (Based on ab Initio Calculations)													
AI level of theory	MP2		UHF			RHF		B3LYP		HF		MP2	
AI basis set	6-31G(d,p)		6-31G(d)			6-31G(d)		6-311+G(d)		6-31G(d,p)		cc-pVTZ(-f)	
partial charges	DMA		RESP			CHelpG		CHelpG		ESP		CHelpG	
		m[a]	av	a[a]	m[a]	av	a[b]	m[b]	av	a[b]	m[b]	av	a[b]	
Ring Atoms													
N_A	**−27**	7	**4**	2	13	**10**	7	13	**12**	11	24	**15**	7	**15**
C_R	41		3						6			−6		−11
($C_R + H_A$)	**50**		**25**			**23**			**23**			**18**		**10**
H_A	10		22						18			24		21
C_W	11	−15	−18	−21				−14	−18	−22	−28	−20	−12	−13
($C_W + H_A$)	**20**	9	**7**	4	4	**6**	10	4	**2**	−1	−2	**5**	12	**7**
H_A	9	24	25	26				18	19	21	26	24	24	21
Side-Chain Atoms														
C_1	12	−16	−9	−2				−16	−4	9	−33	−25	−17	−17
($C_1 + 3H_1$)	**31**	23	**24**	25		**22**		17	**19**	24	17	**22**	26	**22**
H_1	6	13	11	9				11	8	5	17	16	14	13
C_E	−6		−8											−5
($C_E + 3H_C$)	**8**		**9**											**13**
H_C	5		6											6
C_2			3						−12					1
($C_2 + 2H_C$)			**7**			**12**			**−7**		no data, OLPS ?			**13**
H_C			2						3					6
C_S			5						26					−12
($C_S + 2H_C$)			**8**			**12**			**13**		no data, OLPS ?			**0**
H_C			2						−6					6
C_T			−16						−21			0		−18
($C_T + 3H_C$)		-	**1**			**−5**			**−4**			12		**0**
H_C			5						6			4		6

[a] All numbers are percentage values of the charge of one proton. [b] The m and a labels refer to atoms on the side of the methyl and alkyl side chains, repectively.

sufficiently large cutoff distance, several cells were stacked together to form a sufficiently large and well proportioned simulation box, with cutoff distances ranging 12.5−16 Å. Long-range corrections were applied beyond the cutoff distance and the Ewald method was implemented to take into account the long-range character of the electrostatic interactions. The initial position, orientation and conformation of each molecule within the simulation box was the one defined by the lattice coordinates at the CCDB. Because the overall size of the simulation box is defined by the dimensions of the unit cell of each crystal, simulations with different box sizes and cutoff distances were run to check that the dimensions of the simulation box/cutoff were sufficiently large to make negligible any finite size effects. The simulation details for each crystal are given in Table 6.

The simulations were performed using a Nosé−Hoover thermostat coupled with an anisotropic Hoover barostat that allowed the simulation box to change volume and shape under $N-p-T$ conditions. The temperature was fixed to match those used during the crystallographic experiments, and the pressure was set to a null value. All runs were allowed to equilibrate for a period of 100 ps, followed by production times of 200 ps. These simulation times were found appropriate because we start from known configurations close to the equilibrium structure, and it is observed that the relaxation is complete before the end of the equilibration period.

The objective of these simulations is not to test the ability of the present force field to generate the corresponding experimental crystal lattice, a procedure that is still controversial even for simple molecular crystals, but simply to check if they are compatible. The stringency of the test was confirmed with simulation runs where ad hoc parameters were introduced and large distortions of the unit cell paramenters of the lattice observed. The use of an anisotropic barostat coupled with the system allows for a relatively short equilibration period due to the frequent rescaling of the position of the particles. The rather short but effective relaxation time was also confirmed by monitoring the length of the sides and angles of the simulation box as the simulation proceeded through the equilibration period.

Liquid Phase. The ionic liquids simulated were the combinations of $emim^+$, $bmim^+$, and $hmim^+$ with PF_6^-, NO_3^-, and Cl^-. For ionic liquids containing $hmim^+$, simulations were performed in periodic cubic boxes containing 200 pairs of ions, whereas for $emim^+$ and $bmim^+$, 250 pairs were considered. Spherical cutoff distances were defined at 11, 12, and 13 Å for the $emim^+$, $bmim^+$, and $hmim^+$ salts, respectively. Tail corrections to short-range interactions were included, and the long-range electrostatic term was dealt with by the Ewald summation method. The equilibration period in the liquid phase simulation runs is very important. Initially, the ions are placed at random in the simulation box, and the equilibration starts by a short relaxation of a few picoseconds at 1 K and constant $N-V-E$. Then an equilibration period is imposed at the final temperature of the simulation, followed by the activation of the thermostat and barostat. Production runs were started after equilibrations of at least 200 ps.

Production runs of 300 ps were made in $N-p-T$ conditions, under a pressure of 1 bar, and at 298 K for all simulations except for [bmim][NO_3], where the system was simulated at 313 K to compare the results with experimental values at the same

TABLE 6: Crystallographic Data (Space Group Symmetry (sg), Unit Cell Parameters, Density) of the High and Intermediate Melting Point Temperature IL Salts (Crystalline Phases) Simulated in This Work[a]

	salt				
	[mmim][Cl]	[emim][Cl]	[emim][NO_3]	[emim][PF_6]	[ddmim][PF_6]
	Crystallographic References				
CCDBref	JUFBUH[30]	VEPFOL[31]	KUCPED[25]	HAYBUE[23]	HIWNOQ[22]
space group	14b	19	14b	14c	14a
	Simulation Details				
no. of simul. pairs	192	144	96	192	72
no. of stacked cells[a]	4 × 4 × 3	3 × 3 × 1	6 × 2 × 2	4 × 4 × 3	3 × 3 × 2
cutoff (Å)	13.5	13.5	12.5	16	13.5
temp (K)	203	298	298	298	123
	Crystallographic versus Simulated Data				
a (Å)	8.652	10.087	4.540	8.757	9.175
	8.95	**10.13**	**4.56**	**8.82**	**9.10**
b (Å)	7.858	11.179	14.820	9.343	9.849
	7.75	**11.07**	**14.1**	**9.20**	**9.75**
c (Å)	10.539	28.773	13.445	13.701	22.197
	10.3	**28.8**	**13.4**	**13.6**	**23.6**
β (deg)	106.34	90	95.74	103.05	94.132
	108.9	**90.0**	**93.1**	**102.3**	**93.0**
V (Å^3)	687.58	3240.0	899.4	1092.0	2000.6
	698	**3228**	**860**	**1083**	**2081**
ρ (mol dm^{-3})	9.660	8.200	7.385	6.083	3.320
	9.49 ± 0.02	**8.23 ± 0.03**	**7.73 ± 0.05**	**6.13 ± 0.03**	**3.19 ± 0.07**
$\delta\rho$ (%)	−1.8	+0.4	+4.7	+0.8	−3.9
U (kJ mol^{-1})	**−438.8 ± 0.5**	**−431.4 ± 0.9**	**−412.0 ± 1.2**	**−367.8 ± 0.6**	**−402 ± 2**

[a] The simulation results are shown in bold below each experimental datum. The last entry refers to the simulated configurational internal energy of the condensed phase, *U*.

TABLE 7: Density Data for the Intermediate and Low Melting Temperature IL Salts (Liquid Phases) Simulated in This Work

	salt								
	[emim][PF_6]	[emim][NO_3]	[emim][Cl]	[bmim][PF_6]	[bmim][NO_3]	[bmim][Cl]	[hmim][PF_6]	[hmim][NO_3]	[hmim][Cl]
exp method	unknown[34]			picnometry[32]	picnometry[33]	gravimetry[34]	picnometry[32]		gravimetry[34]
ρ (mol dm^{-3})	6.013[a]			4.796	5.710 ± 0.035	6.183	4.186		5.081
	5.669 ± 0.006	**7.317 ± 0.015**	**7.666 ± 0.015**	**4.705 ± 0.005**	**5.780 ± 0.012[b]**	**6.000 ± 0.018**	**4.055 ± 0.004**	**4.846 ± 0.010**	**4.938 ± 0.015**
$\delta\rho$ (%)	−5.7[a]			−1.9	+1.2	−3.0	−3.0		−3.0
U (kJ mol^{-1})	**−352.9 ± 0.1**	**−401.3 ± 0.4**	**−403.8 ± 0.3**	**−335.9 ± 0.8**	**−380.7 ± 0.3**	**−387.3 ± 0.5**	**−359.1 ± 0.6**	**−405.5 ± 0.4**	**−410.0 ± 0.6**

[a] The simulation results are shown in bold below the corresponding experimental datum. The simulated configurational internal energy of the condensed phase, *U*, is also show. [b] Experimental liquid density without reference to the temperature at which the measurement was performed. Probably above the reported melting point temperature of 331−333 K. [c] Experimental and simulation results obtained at 313 K.

temperature. Simulation and relevant experimental data are presented in Table 7.

4. Discussion

The density results shown in Tables 6 and 7 exhibit relative deviations from the corresponding experimental values of the order of a few units of percent (1−5%). These deviations are of the same order of magnitude as those obtained by other authors when comparing the performance of their models against experimental density data.[2,3,4,5,7] In our case we used the same framework to calculate the density of fourteen different ionic liquids, of which nine could be compared against experimental data, in both the liquid and crystalline phases. The results are consistent along the imidazolium cation family (C1, C2, C4, C6, and C12) with three different anions. The level of agreement is very good considering that the calculations are purely predictive: all parameters used were either taken as such from the OPLS-AA/AMBER force field or calculated ab initio; none was adjusted to match experimental data.

The structural properties of the crystals considered in the present study were also correctly predicted by the model. After relaxation, all crystallographic parameters were reproduced within uncertainties corresponding to a few tenths of an ångstrom (except for ddmim$^+$ where deviations are somewhat larger) in the length of the sides of the unit cells and up to 2° in the β director angle of the monoclinic crystals.

At this point we think that the discussion of other results obtainable by simulation with the present model (structural data obtained via the calculation of radial distribution functions, density as a function of temperature or pressure, ionic self-diffusion coefficients or even the internal energy of the system) is unwarranted due to the scarcity or inexistence of reliable and direct experimental results. This means that though the volumetric behavior of the ILs of the imidazolium family is correctly captured by our model, the properties closely related to energetic characteristics are difficult to validate at present. The former are connected to structural characteristics of the present force field that seem to be soundly established, whereas the latter depend significantly on the attribution of electrostatic interaction sites where a complete answer has yet to be formulated. In the present effort we sought to contribute to the discussion of this problem by providing a complete set of atomic partial charges from ab initio calculations including electron correlation on an extended basis set.

As such, the present model can be regarded as a step toward a general force field for ILs of the imidazolium family that was built in a coherent way, is easily integrated with OPLS-AA/AMBER, is transferable between different combinations of cation/anion and was validated against available solid and liquid

state properties. The extension of the present force field to other IL families, namely, imidazolium cations substituted with nonalkyl side chains, would require the calculation of new intramolecular and charge distribution parameters using an ab initio/MD methodology similar to the one employed in this work. Additional work on the parametrization of anions (the ones discussed in this work and others that are becoming quite common in ILs) is also a goal for the future.

Acknowledgment. We are grateful for the financial support of the GRICES/CNRS Portuguese-French cooperation program, a POCTI 34955/99 FCT grant (Portugal), and access to computing facilities at IDRIS and CINES centers in France.

References and Notes

(1) Welton, T. *Chem. Rev.* **1999**, *99*, 2071.
(2) Hanke, C. G.; Price S. L.; Lynden-Bell, R. M. *Mol. Phys*. **2001**, *99*, 801.
(3) de Andrade, J.; Böes, E. S.; Stassen, H. *J. Phys. Chem. B* **2002**, *106*, 3546.
(4) Shah, J. K.; Brennecke, J. F.; Maginn, E. J. *Green Chem.* **2002**, *4*, 112.
(5) de Andrade, J.; Böes, E. S.; Stassen, H. *J. Phys. Chem. B* **2002**, *106*, 13344.
(6) Margulis, C. J.; Stern, H. A.; Berne, B. J. *J. Phys. Chem. B* **2002**, *106*, 12017.
(7) Morrow, T. I.; Maginn, E. J. *J. Phys. Chem. B* **2002**, *106*, 12807.
(8) Jorgensen, W. L.; Maxwell, D. S.; Tirado-Rives, J. *J. Am. Chem. Soc.* **1996**, *118*, 11225; Kaminski, G.; Jorgensen, W. L. *J. Phys. Chem*. **1996**, *100*, 18010.
(9) Cornell, W. D.; Cieplak, P.; Bayly, C. I.; Gould, I. R.; Merz, K. M.; Ferguson, D. M.; Spellmeyer, D. C.; Fox, T.; Caldwell, J. W.; Kollman, P. A. *J. Am. Chem. Soc.* **1995**, *117*, 5179. Parameters obtained from file parm99.dat corresponding to AMBER versions 1999 and 2002.
(10) Harder, S. *Chem. Eur. J.* **1999**, *5*, 1852.
(11) Signorini, G. F.; Barrat, J.-L.; Klein, M. *J. Chem. Phys.* **1990**, *92*, 1294.
(12) Tosi, M. P.; Fumi, G. *J. Phys. Chem. Solids* **1964**, *25*, 45.
(13) Watkins, E. K.; Jorgensen, W. L. *J. Phys. Chem. A* **2001**, *105*, 4118.
(14) Frisch, M. J.; Trucks, G. W.; Schlegel, H. B.; Scuseria, G. E.; Robb, M. A.; Cheeseman, J. R.; Zakrzewski, V. G.; Montgomery, J. A., Jr.; Stratmann, R. E.; Burant, J. C.; Dapprich, S.; Millam, J. M.; Daniels, A. D.; Kudin, K. N.; Strain, M. C.; Farkas, O.; Tomasi, J.; Barone, V.; Cossi, M.; Cammi, R.; Mennucci, B.; Pomelli, C.; Adamo, C.; Clifford, S.; Ochterski, J.; Petersson, G. A.; Ayala, P. Y.; Cui, Q.; Morokuma, K.; Salvador, P.; Dannenberg, J. J.; Malick, D. K.; Rabuck, A. D.; Raghavachari, K.; Foresman, J. B.; Cioslowski, J.; Ortiz, J. V.; Baboul, A. G.; Stefanov, B. B.; Liu, G.; Liashenko, A.; Piskorz, P.; Komaromi, I.; Gomperts, R.; Martin, R. L.; Fox, D. J.; Keith, T.; Al-Laham, M. A.; Peng, C. Y.; Nanayakkara, A.; Challacombe, M.; Gill, P. M. W.; Johnson, B.; Chen, W.; Wong, M. W.; Andres, J. L.; Gonzalez, C.; Head-Gordon, M.; Replogle, E. S.; Pople, J. A. *Gaussian 98*, revision A.10; Gaussian, Inc., Pittsburgh, PA, 2001.
(15) Dunning, T. H., Jr. *J. Chem. Phys*. **1989**, *20*, 1007.
(16) Wang, J.; Cieplak, P.; Kollman, P. A. *J. Comput. Chem*. **2000**, *21*, 1099.
(17) Pádua, A. A. H. *J. Phys. Chem. A* **2002**, *106*, 10116.
(18) Friesner, R. A.; Murphy, R. B.; Beachy, M. D.; Ringnalda, M. N.; Pollard, W. T.; Drunietz, B. D.; Cao, Y. *J. Phys. Chem. A* **1999**, *103*, 1913.
(19) Smith, W.; Forester, T. R. *The DL_POLY package of molecular simulation routines*, *version 2.12*; The Council for The Central Laboratory of Research Councils: Daresbury Laboratory, Warrington, UK, 1999.
(20) Brenneman, C. M.; Wiberg, J. *J. Comput. Chem.* **1987**, *8*, 894.
(21) Hitchcock, P. B.; Lewis, R. J.; Welton, T. *Polyhedron* **1993**, *12*, 2039.
(22) Gordon, C. M.; Holbrey, J. D.; Kennedy, A. R.; Seddon, K. R. *J. Mater. Chem.* **1998**, *8*, 2627.
(23) Fuller, J.; Carlin, R. T.; De Long, H. C.; Haworth, D. *J. Chem. Soc., Chem. Commun*. **1994,** 299.
(24) Kaminski G.; Jorgensen, W. L. *J. Chem. Soc*., *Perkin Trans 2* **1999**, 2365.
(25) Wilkes, J. S.; Zaworotko, M. J. *J. Chem. Soc*., *Chem. Commun*. **1992**, 965.
(26) Vöhringer, G.; Richter, J. *Z. Naturforsch.* **2001**, *56a*, 337.
(27) Rizzo, R. C.; Jorgensen, W. L. *J. Am. Chem. Soc.* **1999**, *121*, 4827.
(28) McDonald, N. A.; Jorgensen, W. L. *J. Phys. Chem. B* **1998**, *102*, 8049.
(29) Weiner, S. J.; Kollman, P. A.; Nguyen D. T.; Case, D. A. *J. Comput. Chem.* **1986**, *7*, 230.
(30) Arduengo, A. J., III; Dias, H. V. R.; Harlow, R. L.; Kline, M. *J. Am. Chem. Soc.* **1992**, *114*, 5530.
(31) Dymeck, C. J., Jr.; Grossie, D. A.; Fretini, A. V.; Adams, W. W. *J. Mol. Struct.* **1989**, *213*, 25.
(32) Chung, S.; Dzyuba, S. V.; Bartsch, R. A. *Anal. Chem.* **2001**, *73*, 3737.
(33) Blanchard, L. A.; Gu, Z.; Brennecke, J. F. *J. Phys. Chem B* **2001**, *105*, 2437.
(34) Huddleston, J. G.; Visser, A. E.; Reichert, W.; Wilauer, M.; Heather, D.; Brocker, G. A.; Rogers, R. D. *Green Chem.* **2001**, *3*, 156.